

unlike Ni(pc)I. Generally a nonmetallic molecular conductor exhibits an exponential temperature dependence of  $\sigma(T)$  because the carrier density or mobility or both are activated. However, Co(pc)I shows an unprecedented, approximately linear variation of  $\sigma(T)$  with temperature.

### Discussion

Co(pc)I is a molecular conductor analogous to the platinum chain conductors rather than to other M(pc)I systems. Indeed Co(pc)I appears to be the first authenticated metal-spine molecular conductor that is not based on a platinum complex, and the conductivity is high even though the Co-Co spacing is 3.12 Å as opposed to the shorter spacings in the platinum-based conductors ( $\leq 2.95$  Å). Nevertheless, the room-temperature conductivity of Co(pc)I is much less than that of the  $\pi$ -orbital conductor, Ni(pc)I. Moreover, although the exact form of  $\sigma(T)$  for Co(pc)I is not understood, the nonmetallic behavior, with  $\sigma(T) \rightarrow 0$  as  $T \rightarrow 0$ , is qualitatively in agreement with the inference drawn from the thermopower and reflectivity measurements that this material is unlike Ni(pc)I in that it shows a gap in the electronic band structure at the Fermi energy.

Although several factors associated with one-dimensional conductors can contribute to the formation of a gap,<sup>25</sup> we consider that the potentials set up by the iodine substructure are the most prominent, and that the difference between Co(pc)I and Ni(pc)I can be understood by considering the influence of the iodine substructure on electronic bands that have different occupancies in the two conductors.

A channel formed by M(pc) stacks in the M(pc)I structure contains a chain of iodine atoms that is trimerized to form a chain

of regular  $I_3^-$  species. The electrostatic potential from such a chain tends to create a gap in the conduction band at an energy level corresponding to  $1/3$  and  $2/3$  filling (Figure 4). However, as noted above, oxidation of Ni(pc) to form Ni(pc)I leads to a  $5/6$  filled  $\pi$  molecular orbital band, whereas Co(pc)I contains a  $1/3$  filled Co( $d_{z^2}$ ) band. Thus, gap formation in Ni(pc)I would have little effect on  $\sigma$ , whereas for Co(pc)I it would tend to cause nonmetallic behavior, as observed. Moreover, one would not expect Co(pc)I to exhibit a well-defined gap and typical semiconductive behavior. The iodine chains in the M(pc)I, though individually ordered, are disordered with respect to each other. Thus, we take the anomalous temperature response to  $\sigma(T)$  for Co(pc)I to reflect a gap at the Fermi surface that is smeared out because the Co(pc) stacks are subject to a random potential from the disordered iodine chains.

In summary, the entire set of differences between Co(pc)I and Ni(pc)I can be discussed self-consistently by treating the former to be a metal-spine conductor, whereas carriers on the latter are associated with the pc ring.

**Acknowledgment.** The work at Northwestern University was supported by the Northwestern University Materials Research Center under the National Science Foundation NSF-MRL program (Grant DMR 82-16972) and through the Solid State Chemistry Program of the National Science Foundation (DMR8116804 to B.M.H.). The authors thank Dr. S. M. Palmer for Resonance Raman measurements.

**Registry No.** Co(pc)I, 30289-99-7.

**Supplementary Material Available:** Tables III (positions and anisotropic thermal parameters for non-hydrogen atoms; hydrogen atom positions and isotropic thermal parameters) and IV (structure amplitudes) for Co(pc)I (4 pages). Ordering information is given on any current masthead page.

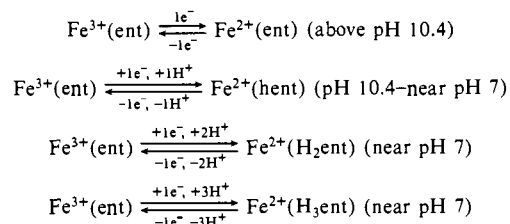
(25) (a) Jerome, D.; Schulz, H. J. In "Extended Linear Chain Compounds"; Miller, J. S., Ed.; Plenum Press, New York, 1982; Vol 2, pp 159-204. (b) Comès, R.; Lambert, M.; Launais, H.; Zeller, H. R. *Phys. Rev. B: Solid State* 1973, 8, 571-575.

## The pH-Dependent Reduction of Ferric Enterobactin Probed by Electrochemical Methods and Its Implications for Microbial Iron Transport<sup>1</sup>

Chi-Woo Lee, David J. Ecker, and Kenneth N. Raymond\*

Contribution from the Department of Chemistry, University of California, Berkeley, California 94720. Received March 4, 1985

**Abstract:** The coordination chemistry of ferric enterobactin has been probed by cyclic voltammetry, normal and differential pulse polarography, and controlled-potential electrolysis. The formal potential of the iron(3+/2+) couple for the enterobactin complex is found to be -1.03 V vs. SSCE (-0.79 V vs. NHE) at pH 7.4 in a solution containing 0.4 M NaClO<sub>4</sub> and 20 mM phosphate buffer. The first protonation constant of ferric enterobactin is 10<sup>4.8</sup>; therefore in the pH range studied (6-11.4) ferric enterobactin is present entirely as [Fe(ent)]<sup>3-</sup>. Thus the pH dependence of the formal potentials in this region is due entirely to protonation of the *ferrous* complex. Four regions involving one-electron transfers have been identified. These reactions are



The implications of these data for the mechanism of enterobactin-mediated iron transport in microorganisms which utilize this siderophore are presented.

Enterobactin is a siderophore (microbial iron transport agent) whose coordination chemistry<sup>2-6</sup> and mechanism(s) of microbial

iron transport<sup>7-9</sup> have been of recent interest, largely because of the important role iron availability plays in bacterial growth and

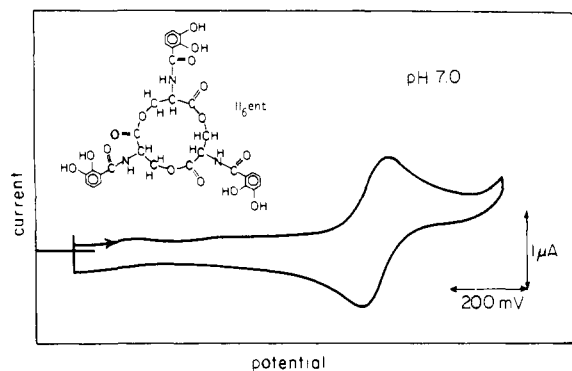


**Figure 1.** Cyclic voltammogram of 0.2 mM  $\text{Fe}^{3+}(\text{ent})$  in 2 M  $\text{NH}_4\text{Cl}$  at pH 7.0 (20 mM phosphate). Negative potentials (vs. sodium chloride saturated calomel electrode, SSCE) are plotted to the right and reduction currents are plotted upward. Area of working electrode (HMDE) 0.032  $\text{cm}^2$ ; initial potential  $-0.20$  V; scan rate  $0.1$  V  $\text{s}^{-1}$ .

pathogenicity. Due to the enormous stability of the ferric complex ( $K_f \approx 10^{52}$ )<sup>6</sup> and its specificity (the ferrous ion is only weakly complexed), the  $\text{Fe}(3+/2+)$  formal potential of the enterobactin complex is highly negative (reported earlier as  $-0.986$  V (vs. NHE) at pH 10).<sup>6,10</sup> However, the full coordination of  $\text{Fe}^{3+}$  by all three catecholate groups of enterobactin requires the loss, at neutral pH, of six protons. Thus there is a strong dependence of the stability of the ferric enterobactin complex, and its reduction potential, on pH. We previously estimated the potential at pH 7.4 to be  $-0.75$  V (vs. NHE) from solution studies of the ferric complex<sup>6</sup> and suggested that the reported hydrolysis of the ligand accompanying iron transport<sup>11,12</sup> was required to allow in vivo reductive removal of iron by physiological reductants.<sup>10</sup> However, recent studies<sup>7,4,8</sup> have not supported this model, leaving as one possibility that iron is ultimately removed from the enterobactin complex by reduction in a low-pH medium. Thus the pH dependence of the ferric enterobactin reduction potential has taken on renewed significance.

We report here the electrochemistry of the ferric enterobactin complex from pH 6 to 11.4. Since the first protonation constant of  $[\text{Fe}(\text{ent})]^{3-}$  is  $10^{4.8}$ ,<sup>6</sup> this complex is the only  $\text{Fe}(\text{III})$ -containing species present in significant concentration over the pH range studied. The pH dependence of the formal potential can therefore be used to determine the protonation constants of the ferrous complexes as well as determining the feasibility of biochemical reduction.

## Experimental Section

Conventional electrochemical instrumentation, cells, and electrodes were employed for the cyclic voltammetric, polarographic, and con-

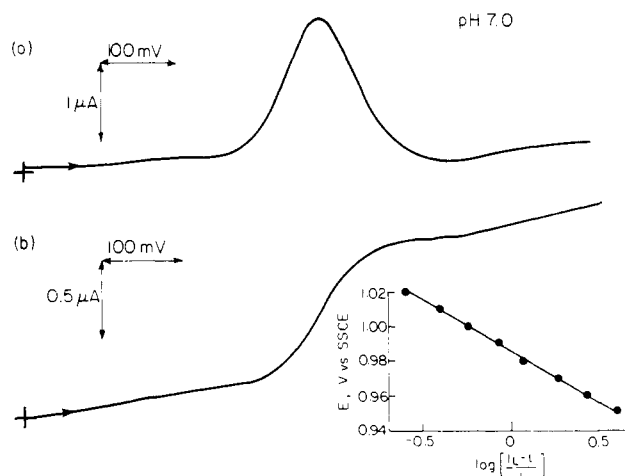


**Figure 2.** (a) Differential pulse polarogram of 0.2 mM  $\text{Fe}^{3+}(\text{ent})$  in 0.4 M  $\text{NaClO}_4$  solution at DME. Flow rate  $1.2 (\pm 0.1)$   $\text{mg s}^{-1}$ ; initial potential  $-0.60$  V; scan rate  $5$   $\text{mV s}^{-1}$ ; pulse amplitude  $25$  mV. Other conditions are the same as in Figure 1. (b) Normal pulse polarogram. Conditions are the same as in (a). The inset shows  $-E$  vs.  $\log [(iL - i)/i]$  for the normal pulse polarogram.

**Table I.** Stability and Protonation Constants of Ferric and Ferrous Enterobactin

reaction	$\log K, \text{Fe}^{3+ a,b}$	$\log K, \text{Fe}^{2+ c}$
$\text{M} + \text{H}_6\text{ent} \rightarrow \text{M}(\text{ent}) + 6\text{H}^+$	-9.7	-39.5
$\text{M}(\text{ent}) + \text{H}^+ \rightarrow \text{M}(\text{Hent})$	4.80	10.4 (2)
$\text{M}(\text{Hent}) + \text{H}^+ \rightarrow \text{M}(\text{H}_2\text{ent})$	3.15	7.7 <sup>d</sup>
$\text{M}(\text{H}_2\text{ent}) + \text{H}^+ \rightarrow \text{M}(\text{H}_3\text{ent})$		7 <sup>d</sup>

<sup>a</sup> From ref 6. <sup>b</sup> At ionic strength 0.1 M. <sup>c</sup> At ionic strength 0.4 M. <sup>d</sup> The sum of  $\log K_2$  and  $\log K_3$  is well determined. For  $\beta_n = [\text{H}_n\text{Fe}^{11}(\text{ent})]/[\text{Fe}^{11}(\text{ent})][\text{H}^+]^n$   $\log \beta_3 = 25.0$  (2). The correlation coefficient between  $\log \beta_1$  and  $\log \beta_3$  from the least-squares refinement is 0.7. The equation fit in the least-squares process is  $E = E^0 + 0.059 \log \alpha$ , where  $\alpha = 1 + \beta_1[\text{H}^+] + \beta_2[\text{H}^+]^2 + \beta_3[\text{H}^+]^3$ .

trolled-potential coulometric measurements.<sup>10,13,14</sup> Quoted potentials are with respect to the NHE. Experiments were conducted at the laboratory temperature,  $22 \pm 2$  °C.

All chemicals were reagent grade and were used as received. Enterobactin was isolated as described before.<sup>7,15</sup> The sample used in Figure 1 is the  $\text{Fe}^{3+}(\text{ent})$  fraction directly from the DEAE column in aqueous ammonium chloride. The sample prepared from isolated enterobactin and ferric chloride in the sodium perchlorate medium gives electrochemical results identical with those such as shown in Figure 2. Analytically pure enterobactin and solid ferric chloride hexahydrate, carefully weighed, were added sequentially in one-to-one ratio to buffered pH 7.0 solution. Greater than 95% complex formation was achieved, based on the absorbance ( $\epsilon_{495}$  5600  $\text{M}^{-1} \text{cm}^{-1}$ ). The solution volume was decreased to the desired experimental concentrations by evaporation under reduced pressure at 30–40 °C. A Gelman Acrodic<sup>R</sup> filter (0.2  $\mu\text{m}$ ) was utilized to filter the final solution. Previous unsuccessful attempts to examine the electrochemistry at physiological pH are apparently due to the borate buffer added.<sup>16</sup> The measurements were done as quickly as possible at high pH (<5 min at pH 11.4, the highest pH used). For the higher pH samples additional peaks due to lactone hydrolysis products of ferric enterobactin become increasingly apparent, but even at the highest pH the sample peak clearly could be seen.

## Results

Figure 1 shows the cyclic voltammogram (CV) recorded with 0.2 mM  $[\text{Fe}^{3+}(\text{ent})]^{3-}$  in an aqueous ammonium chloride electrolyte solution at pH 7.0, using a hanging mercury drop electrode (HMDE) as working electrode with a platinum wire counter electrode in the usual two-compartment cell. The peak current

(1) Paper 34 in the series "Coordination Chemistry of Microbial Iron Transport Compounds". The previous paper in this series is: Chung, T. D. Y.; Matzanke, B. F.; Winkelmann, G.; Raymond, K. N. *J. Bacteriol.*, submitted for publication.

(2) Raymond, K. N.; Müller, G.; Matzanke, B. F. *Top. Curr. Chem.* **1984**, *123*, 50–102.

(3) Neilands, J. B. *Annu. Rev. Microbiol.* **1982**, *36*, 285–309.

(4) Pecoraro, V. L.; Harris, W. R.; Wong, G. B.; Carrano, C. J.; Raymond, K. N. *J. Am. Chem. Soc.* **1983**, *105*, 4623–4633.

(5) Pecoraro, V. L.; Wong, G. B.; Kent, T. A.; Raymond, K. N. *J. Am. Chem. Soc.* **1983**, *105*, 4617–4623.

(6) Harris, W. R.; Carrano, C. J.; Cooper, S. R.; Sofen, S. R.; Avdeef, A.; McArdle, J. V.; Raymond, K. N. *J. Am. Chem. Soc.* **1979**, *101*, 6097–6104.

(7) Ecker, D. J.; Matzanke, B. F.; Raymond, K. N. *J. Bacteriol.*, submitted for publication.

(8) Heidinger, S.; Braun, V.; Pecoraro, V. L.; Raymond, K. N. *J. Bacteriol.* **1983**, *153*, 109–115.

(9) Plaha, D. S.; Rogers, H. J. *Biochim. Biophys. Acta* **1983**, *760*, 246–255.

(10) Cooper, S. R.; McArdle, J. V.; Raymond, K. N. *Proc. Natl. Acad. Sci. U.S.A.* **1978**, *75*, 3551–3554.

(11) O'Brien, I. G.; Cox, G. B.; Gibson, F. *Biochim. Biophys. Acta* **1971**, *237*, 537–549.

(12) Langman, L.; Young, I. G.; Frost, G. E.; Rosenberg, H.; Gibson, F. *J. Bacteriol.* **1972**, *112*, 1142–1149.

(13) Paffett, M. T.; Anson, F. C. *Inorg. Chem.* **1983**, *22*, 1347–1355.

(14) Lee, C.-W.; Anson, F. C. *Inorg. Chem.* **1984**, *23*, 837–844.

(15) Young, I. G.; Gibson, F. "Methods in Enzymology"; Fleischer, S., Packer, L., Eds.; Academic Press: New York, 1979; Vol. LV1, pp 394–398.

(16) Waite, J. H. *Anal. Chem.* **1984**, *56*, 1935–1937 and references therein.

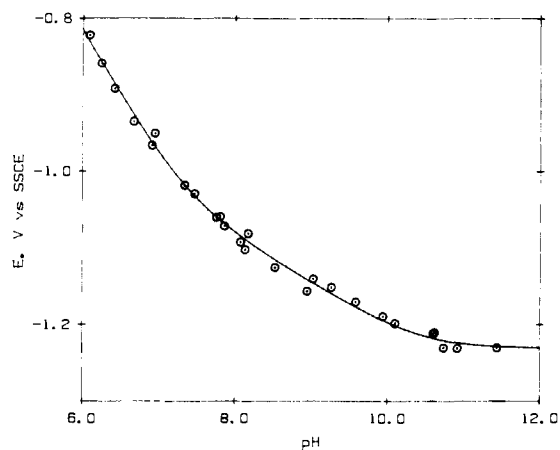
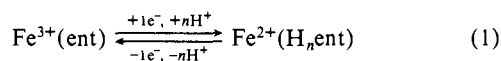


**Figure 3.** pH dependence of formal potentials of iron(3+,2+) enterobactin complexes. Buffers used were 20 mM bicarbonate (above pH 9), 50 mM tris[(hydroxymethyl)amino]methane hydrochloride (pH 9–7) and 20 mM phosphate (pH 8–6); all solutions contained 0.4 M NaClO<sub>4</sub>. The line is the theoretical curve calculated from the constants determined from the least-squares refinement (Table I).

( $i_p$ ) vs. the square root of the scan rate ( $\nu^{1/2}$ ) is linear with zero intercept, indicating that the electron-transfer rate is controlled by mass transfer.<sup>17</sup> The fact that the ratio of cathodic and anodic peak currents is 1.0 suggests that the ferrous complex formed in the electroreduction is stable within the CV time scale used. Controlled-potential electrolysis confirms that the number of electrons involved is 1. Thus the well-defined CV wave pair of peak separation ( $E_{pc} - E_{pa}$ ) near 60 mV is due to a one-electron, diffusion-controlled process for which the formal potential can be evaluated by taking the average of the cathodic and anodic peak potentials [ $(E_{pc} + E_{pa})/2$ ].

Other support for a one-electron, Nernstian reaction comes from the pulse polarographic results at the dropping mercury electrode (DME) shown in Figure 2. The log plot of a normal pulse polarogram is linear with a slope of near -60 mV. The formal potential is more easily discernible from the differential pulse polarogram.<sup>17</sup>

Since the only Fe(III)-containing species present in the pH range studied is  $[\text{Fe}(\text{ent})^{3-}]$ , the reaction is assigned to be



on the basis of the electrochemical results, where  $n$  depends upon the pH. The pH dependence of the formal potential is shown in Figure 3. There is one clear break corresponding to a protonation reaction which occurs at pH 10.4 and two overlapping protonation reactions near pH 7. Nonlinear least-squares refinement of these data gave the protonation constants presented in Table I. The slope of the  $E$  vs. pH curve (Figure 3) is  $\sim 0$  mV above pH 10.4 (0 protons in the redox process) and 55 mV/pH unit below 10.4 (1 proton) and then gradually changes from -55 to -188 mV/pH unit (3 protons). The two- and three-proton reactions have protonation constants sufficiently close as to make their independent determination relatively uncertain (i.e.,  $K_2$  is near or less than  $K_3$ ). It is their product that is well determined (i.e., there is little correlation between  $\log \beta_3$  and  $\log \beta_1$ ).

**Implications for *E. coli* Iron Transport Mediated by Enterobactin.** The biochemical implications of the present results can be summarized by the potentials. In excellent agreement with our earlier report,<sup>6,10</sup> we find the high-pH limit for the reduction potential of ferric enterobactin to be -0.99 V (vs. NHE). Much more important is the measured potential at physiological pH (7.4)

of -0.79 V. This is somewhat more negative than that previously estimated by us.<sup>10</sup> The increasing pH dependence of the potential at low pH further raises the potential to -0.57 V at pH 6. Below this pH protonation of the ferric complex and dissociation of the ferrous complex become significant and the electrochemical reaction is not well defined. However, the previous estimate<sup>4</sup> of the potential as +0.17 V at pH 4, which assumed no complexation of the ferrous ion by enterobactin at this pH, is supported. The protonation constants for the ferrous complex, derived from the data on Figure 3, are shown in Table I. These data show that there is no significant complexation of  $\text{Fe}^{2+}$  by enterobactin at pH 4. Since the periplasmic space of *E. coli* is an acidic compartment of the cell, analogous to the lysosome in mammalian cells,<sup>18,19</sup> and since it appears that this region accumulates ferric enterobactin during the early stages of iron transport<sup>7,20</sup> physiological reduction remains a plausible mechanism for iron release in *E. coli*.

In a series of papers<sup>21–24</sup> Hider, Silver, and co-authors have presented data regarding the coordination chemistry of ferric enterobactin and model catechol complexes which in several respects differ from those presented here. We have shown<sup>25,26</sup> from circular dichroism studies that the preferred chirality at the metal center for ferric enterobactin and its Cr(III) and Rh(III) analogues is  $\Delta$ . We have described the stepwise stability constants of a series of ferric catechol complexes<sup>27</sup> and the stability and protonation equilibria of ferric enterobactin<sup>28</sup> and analogues.<sup>6,29,30</sup> We showed that the protonation of ferric enterobactin occurs in three discrete one-proton steps in aqueous solution, resulting eventually in the neutral complex  $[\text{Fe}^{\text{III}}(\text{H}_3\text{ent})]^0$ . Although Hider et al. once characterized the protonated ferric enterobactin species as the neutral, tetraprotonated ferrous complex  $[\text{Fe}^{\text{II}}(\text{H}_4\text{ent})]^0$  (Figure 2 of their paper<sup>21</sup>), they subsequently modified their view of the stoichiometry of this reaction and proposed<sup>22</sup> a single, three-proton reaction in aqueous solution resulting in an internal redox reaction to give a species characterized as  $[\text{Fe}^{\text{II}}(\text{H}_3\text{ent}^-)]$  (where ent indicates the oxidation of one catechol ring to a semiquinone). We subsequently showed<sup>4</sup> that the Hider et al. data<sup>22</sup> are only consistent with a single-proton reaction. These authors now apparently agree with our assignment of the stoichiometry and species of the aqueous protonation of ferric enterobactin<sup>24</sup> but differ in their view regarding the possibility, suggested by us, that protonation in a region of the cell may sufficiently raise the ferric enterobactin redox potential so as to make this a plausible mechanism for in vivo release of the metal ion. Regarding our proposed protonation/reduction mechanism Hider et al. state:<sup>24</sup> "Bacteria, unlike eukaryotes, possess a single intracellular compartment, and it is extremely unlikely that a bacterium would permit the pH of its cytoplasm to fall to these acidic pH values...". However, this is incorrect: *E. coli*, like other Gram-negative bacteria, has an inner and an outer membrane.<sup>31</sup> The intervening region, which is called the periplasmic space, constitutes up to

(20) Matzanke, B. F.; Huynh, B. H.; Ecker, D. J.; Müller, G.; Raymond, K. N. *J. Bacteriol.*, submitted for publication.

(21) Hider, R. C.; Silver, J.; Neilands, J.; Morrison, I. E. G.; Rees, L. V. C. *FEBS Lett.* **1979**, *102*, 325–328.

(22) Hider, R. C.; Mohd-Nor, A. R.; Silver, J.; Morrison, I. E. G.; Rees, L. V. C. *J. Chem. Soc., Dalton Trans.* **1981**, 609–622.

(23) Hider, R. C.; Howlin, B.; Miller, J. R.; Mohd-Nor, A. R.; Silver, J. *Inorg. Chim. Acta* **1983**, *80*, 51–56.

(24) Hider, R. C.; Bickar, D.; Morrison, I. E. G.; Silver, J. *J. Am. Chem. Soc.* **1984**, *106*, 6983–6987.

(25) Isied, S. S.; Kuo, G.; Raymond, K. N. *J. Am. Chem. Soc.* **1976**, *98*, 1763–1767.

(26) Raymond, K. N.; Abu-Dari, K.; Sofen, S. R. *ACS Sym. Ser.* **1980**, *119*, 133–137.

(27) Avdeef, A.; Sofen, S. R.; Bregante, T. L.; Raymond, K. N. *J. Am. Chem. Soc.* **1978**, *100*, 5362–5370.

(28) Harris, W. R.; Carrano, C. J.; Raymond, K. N. *J. Am. Chem. Soc.* **1979**, *101*, 2213–2214.

(29) Harris, W. R.; Weilt, F. L.; Raymond, K. N. *J. Chem. Soc., Chem. Commun.* **1979**, 177–178.

(30) Harris, W. R.; Raymond, K. N. *J. Am. Chem. Soc.* **1979**, *101*, 6534–6541.

(31) See, for example, Stanier, R. Y.; Adelberg, E. A.; Ingraham, J. L.; Wheelis, M. L. "Introduction to the Microbial World"; Prentice Hall: New York, 1979.

(17) Bard, A. J.; Faulkner, L. R. "Electrochemical Methods"; Wiley: New York, 1980; Chapters 5 and 6.

(18) Stock, J. B.; Rauch, B.; Roseman, S. *J. Biol. Chem.* **1977**, *252*, 7850–7861.

(19) Cramer, W. A.; Dankert, J. R.; Uratani, Y. *Biochim. Biophys. Acta* **1983**, *737*, 173–193 and references cited therein.

40% of the cell volume and, as noted in our earlier discussion of our electrochemical results, is acidic. The *outer* membrane transport protein for ferric enterobactin has been shown to recognize and transport synthetic analogues.<sup>8,7</sup> This apparently delivers the iron complex to the periplasmic space. The steps involved in the subsequent transport of iron into the cytoplasm have yet to be characterized.

### Conclusion

The electrochemical results presented here show that iron removal via protonation and reduction is a possible mechanism for *in vivo* iron transport of *E. coli*. We suggest that this could occur in the periplasmic space of *E. coli*, a region of the organism known to be relatively acidic. While the interpretive issue of the structure of the protonated ferric enterobactin complex ultimately must await unambiguous assignment from an X-ray diffraction study, we believe the weight of evidence supports what we have described as the "salicylate" mode of bonding.<sup>4,5</sup> Factual issues which are now completely definitive are the following:

(1) Ferric enterobactin at or above neutral pH is a tris(catechol)iron(III) complex with a  $\Delta$  chirality.

(2) Protonation of ferric enterobactin, which occurs only below pH 5, is stepwise, in *single*-proton reactions; the first two protonation constants are  $10^{4.8}$  and  $10^{3.15}$ .

(3) Protonation of *ferrous* enterobactin begins at pH 10.4, resulting in the strongly pH-dependent redox potential reported here. The formal electrochemical potentials for iron(III,II) enterobactin are (at pH noted)  $-0.99$  ( $> 10.4$ ),  $-0.79$  (7.4),  $-0.57$  (6.0) V (vs. NHE).

(4) In (or from) aqueous solution, all of the protonated ferric enterobactin species, including the neutral  $[\text{Fe}^{\text{III}}\text{H}_3\text{ent}]^0$ , contain exclusively high-spin iron(III).

**Acknowledgment.** This research is supported by NIH Grant AI 11744. D.J.E. thanks the American Cancer Society for a postdoctoral fellowship.

**Registry No.**  $[\text{Fe}(\text{ent})]^{3-}$ , 61481-53-6; Fe, 7439-89-6.

## Preparation and Conformations of the Medium-Ring Dimethylphosphazenes $(\text{NPMe}_2)_{9-12}$ : Crystal and Molecular Structures of Octadecamethylcyclononaphosphazene, Eicosamethylcyclodecaphosphazene, Docosamethylcycloundecaphosphazene, and Tetracosamethylcyclododecaphosphazene

Richard T. Oakley,<sup>1</sup> Steven J. Rettig, Norman L. Paddock,\* and James Trotter\*

Contribution from the Department of Chemistry, The University of British Columbia, Vancouver, B.C., Canada V6T 1Y6. Received March 6, 1985

**Abstract:** With the extension of the series by the preparation of  $(\text{NPMe}_2)_{9-12}$ , the dimethylphosphazenes form the longest known series of cyclic compounds with full structural characterization. Crystal data for  $(\text{NPMe}_2)_n$  are as follows:  $n = 9$ , triclinic,  $P\bar{1}$ ,  $a = 20.6208$  (10) Å,  $b = 15.2473$  (7) Å,  $c = 13.3132$  (7) Å,  $\alpha = 90.492$  (4)°,  $\beta = 88.516$  (4)°,  $\gamma = 119.740$  (4)°,  $Z = 4$ ,  $R = 0.040$  for 7008 reflections;  $n = 10$ , orthorhombic, *Acam*,  $a = 20.5498$  (11) Å,  $b = 8.1798$  (5) Å,  $c = 23.4152$  (14) Å,  $Z = 4$ ,  $R = 0.035$  for 1124 reflections;  $n = 11$ , triclinic,  $P\bar{1}$ ,  $a = 8.2739$  (7) Å,  $b = 12.533$  (2) Å,  $c = 21.651$  (3) Å,  $\alpha = 86.43$  (1)°,  $\beta = 83.96$  (1)°,  $\gamma = 84.89$  (1)°,  $Z = 2$ ,  $R = 0.033$  for 5589 reflections;  $n = 12$ , triclinic,  $P\bar{1}$ ,  $a = 8.397$  (3) Å,  $b = 12.007$  (4) Å,  $c = 13.390$  (2) Å,  $\alpha = 114.24$  (2)°,  $\beta = 99.57$  (2)°,  $\gamma = 92.97$  (3)°,  $Z = 1$ ,  $R = 0.051$  for 3422 reflections. The mean P-N bond length (1.595 Å) is independent of ring size and is greater than it is in chloro- or fluorophosphazenes, a result of the low electronegativity of the methyl group. The geometry of the  $\text{PC}_2$  group ( $\text{P-C} = 1.808$  Å,  $\text{CPC} = 103.9^\circ$ ) is independent of ring size, but electronic changes within the ring cause the NPN angle to decrease steadily from  $119.8^\circ$  in  $(\text{NPMe}_2)_4$  to  $116.3^\circ$  in  $(\text{NPMe}_2)_{12}$ . The stereochemical effectiveness of the nitrogen lone pairs is reduced by their partial delocalization into  $d\pi$ -orbitals of phosphorus, so that the PNP angles are both large and variable. The conformations, controlled primarily by steric interactions between methyl groups, are related to those of the cycloalkanes, where known, of the same polymeric number. The comparability depends on the weakness of the steric interactions of the nitrogen atoms; systematic differences arise because the  $\text{Me}\cdots\text{Me}$  interactions are net attractive. Although the molecules are flexible in solution, a medium-ring effect, analogous to that in the cycloalkanes, is found in  $(\text{NPMe}_2)_9$ , in which many of the local interactions are of high energy, and also in the probable steric hindrance to the final step in the methylation of the fluoride to  $(\text{NPMe}_2)_{10}$ .

Much of our systematic knowledge of cyclic molecules comes from the study of the cycloalkanes and their derivatives. The difficulties encountered in the synthesis of medium-ring compounds and the dependence of their chemical properties and heats of formation on ring size were early traced to the high torsional barrier to rotation about skeletal bonds and, later, to transannular repulsive interactions. The resultant structural effects have been the subject of numerous investigations.<sup>2</sup>

(1) Present address: Department of Chemistry and Biochemistry, University of Guelph, Guelph, Ontario, Canada N1G 2W1.

(2) For reviews of the chemistry of cycloalkanes, see: Clark, T.; McKervey, M. D. In "Comprehensive Organic Chemistry"; Barton, D. H. R., Ollis, W. D., Eds.; Pergamon Press: Oxford, 1979; Vol I (Stoddart, J. F., Ed.), p 37.

Inorganic cyclic compounds<sup>3</sup> include the various molecular forms of sulfur, the metaphosphates  $(\text{OPO}_2^-)_n$ , the siloxanes

(3) Haiduc, I. "Chemistry of Inorganic Ring Systems"; Wiley-Interscience: New York, 1970. Rheingold, A. L., Ed. "Homoatomic Rings, Chains, and Macromolecules of the Main Group Elements"; Elsevier: Amsterdam, 1977.

(4) Ondik, H. M.; Block, S.; MacGillavry, C. H. *Acta Crystallogr.* **1961**, *14*, 555.

(5) Steinfink, H.; Post, B.; Fankuchen, I. *Acta Crystallogr.* **1955**, *8*, 420.

(6) Fawcett, J. K.; Kocman, V.; Nyburg, S. C. *Acta Crystallogr., Sect. B* **1972**, *B30*, 1979.

(7) Hazekamp, R.; Migchelsen, T.; Vos, A. *Acta Crystallogr.* **1962**, *15*, 539.

(8) Dougill, M. W. *J. Chem. Soc.* **1961**, 5471.

(9) Mijlhoff, F. C. *Acta Crystallogr.* **1965**, *18*, 795.